The Polymerization Mechanism and Kinetics of DGEBA with BF_3–MEA

MICHAEL TACKIE* and GEORGE C. MARTIN

Department of Chemical Engineering and Materials Science, Syracuse University, Syracuse, New York 13244

SYNOPSIS

The diglycidyl ether of bisphenol-A (DGEBA) and boron trifluoride monoethylamine (BF_3–MEA) were used in a model system to investigate the chemical and physical changes that occur during polymerization. Experiments using ^{19}F and ^{1}H nuclear magnetic resonance (NMR) and Fourier transform infrared spectroscopy (FTIR) showed that BF_3–MEA breaks down rapidly into HBF_4 and an amine salt at 85°C and above. The HBF_4 complexes with the epoxy groups, producing an activated monomer that reacts with epoxy in an etherification reaction. A mechanism is proposed whereby activated epoxy sites (complexes) continuously add epoxy throughout the reaction, but where unactivated epoxies (monomer molecules) are unable to react with each other. The reaction rate and mode (kinetic vs. diffusion control) therefore are strongly influenced by the BF_3–MEA concentration and the reaction temperature. © 1993 John Wiley & Sons, Inc.

INTRODUCTION

Epoxy resins are used as adhesives, as barrier films in food packaging, as matrix resins in fiber-reinforced composites, and in a host of other applications. The formulations are usually complex mixtures of one or more epoxies, curing agents, accelerators, and modifiers such as fillers. To understand the curing reaction, a simplified formulation was chosen for this study.

The curing reaction of the diglycidyl ether of bisphenol-A (DGEBA) and boron trifluoride monoethylamine BF_3–MEA was investigated with nuclear magnetic resonance (NMR), Fourier transform infrared spectroscopy (FTIR), differential scanning calorimetry (DSC), gel permeation chromatography (GPC), rheological and dynamic mechanical analyses, and solvent extraction. The purpose of the work was to delineate the reaction mechanism and kinetics of BF_3–MEA/DGEBA, to model the resulting network growth, and to determine if the network growth model and kinetics could be related to the viscosity given the temperature history, reactant concentrations, and processing conditions for the resin. The results of the curing mechanism and kinetics studies will be presented in this paper.

Until recently, the cure of BF_3–MEA/epoxy systems was thought to begin with the electrophilic ring-opening of the epoxy.[1,2] Landau[1] measured the progression in molecular weight in a range of BF_3–ether complexes with extent of reaction and observed that the molecular weight of the reacting mixture reached a maximum at intermediate extents of reaction and then decreased. Landau postulated that the BF_3–MEA complex dissociates with heat, liberating BF_3, which reacts with the epoxy by insertion into the growing chain. The insertion mechanism, although unusual, has been observed in other systems. Edwards et al.[3] observed reaction products similar to those described above in the polymerization of cyclic ether systems with boron trichloride. Similar observations were recorded by Robinson.[4]

Harris and Temin[2] proposed a mechanism that does not involve the breakdown of BF_3–MEA. In their mechanism, a proton from the amine complexes with the oxygen on an epoxy to create an oxygen atom with a slight positive charge:

* To whom correspondence should be addressed at INDSPEC Chemical Corporation, 1010 William Pitt Way, Pittsburgh, PA 15238.

Journal of Applied Polymer Science, Vol. 48, 793–808 (1993)
 CCC 0021-8995/93/050793-16

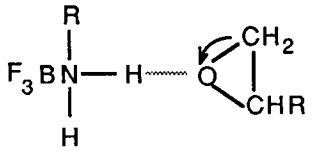

They also proposed an equilibrium reaction between this complex and a secondary oxonium ion:

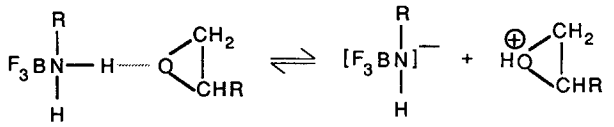

Unlike Landau, they maintained that curing was not caused by some sort of decomposition of the BF_3–MEA, but, rather, by a complex of the epoxy and the BF_3–MEA. The mechanism is very similar to that proposed by Arnold,[5] except that Arnold attributed the catalytic activity of BF_3–MEA to a proton that is liberated from BF_3–MEA by heat.

A modification of the Landau mechanism[6] was widely accepted until very recently. In this mechanism, the epoxy group complexes with BF_3 that is formed by the thermal dissociation of BF_3–MEA. The reaction then proceeds—without the fluorine end-capping of the growing chains—from the cation on the secondary carbon atom of the epoxy:

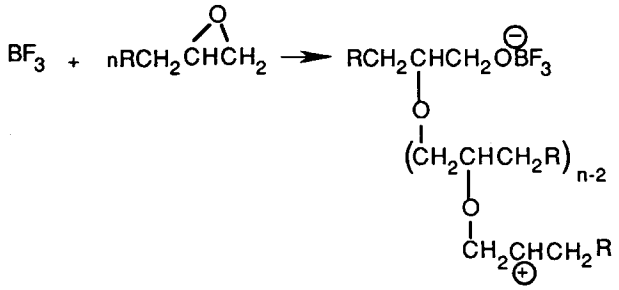

Although there is evidence for the dissociation of BF_3–amine compounds into $-BF_2$- and $-BF_4$-containing species,[7–9] this possibility was largely ignored.

The accepted mechanism[6] has been disputed by Smith et al.[10–12] They provided evidence that BF_3–MEA is hydrolyzed to HBF_4 and its derivatives very early in the cross-linking reaction. The proposed reactions are

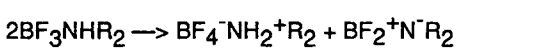

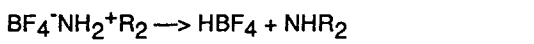

Here, HBF_4, not BF_3–MEA, is the true catalyst. NMR and FTIR spectroscopy were used to monitor the thermal conversion of BF_3–MEA in solution and in tetraglycidyldiaminodiphenyl methane/diaminodiphenyl sulfone (TGDDM/DDS). The results indicate that a rapid thermal conversion of BF_3–MEA to HBF_4 (less than 5 min in duration) occurs in resins where BF_3–MEA is used as an accelerator.

The proposed mechanism of Smith et al. differs from yet another mechanism advanced by Happe et al.[13] Happe et al. heated BF_3–MEA for 1 h at 139°C, and, upon dissolving the sample in DMSO, found no appreciable difference in the proton spectra before and after the heat treatment. They proposed that, above 85°C, BF_3–MEA is slowly converted to a tetrafluoroborate salt with a loss of fluorine. The catalytic species is chemically stable and does not form a complex with the epoxy. Also, they proposed that the salt is a true catalyst, migrating throughout the epoxy catalyzing the cross-linking reactions. The mechanism they suggest is

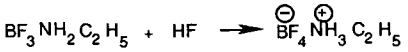

Recently, Chen and Pearce[14] proposed another mechanism where the amine complex donates a proton to the epoxy group to form an oxonium ion, which slowly activates the terminal carbon on the epoxy.

In addition to these mechanisms, Kubisa[15] and Kubisa and Szymanski[16] showed that in the presence of relatively large concentrations of alcohol groups the mechanism of polymerization switches from the "activated chain end" mechanism described here to the "activated monomer" mechanism.

The mechanism of catalyst activation of the epoxy is important for two reasons: First, the mechanism dictates the stoichiometry of the reaction, i.e., how many HBF_4, fluoroborate salt, or other active species are liberated by each mole of BF_3–MEA and when they are liberated. This information is necessary for the correct development of kinetic equations. Second, the breakdown mechanism affects the network modeling fundamentally. The two extremes of a slow release of a mobile catalyst[13] and the almost instantaneous release of an acid[10–12] translate into network structures and properties that are quite different.

EXPERIMENTAL

Materials

BF_3–MEA as obtained from the manufacturer (Alfa Products, Maynard, MA) was 98% pure. It was washed with a 50% solution of methylene chloride in methanol prior to use. Salts of this type (BF_3 complexes) are hygroscopic and they slowly hydrolyze to fluoroborates upon standing. The washing treatment dissolves these hydrolysis products. After washing, the salt was dried in a vacuum oven at 25°C and 20 mmHg for 30 min.

BF_3–MEA/DGEBA samples were prepared for the FTIR experiments by melt-mixing at 85°C. The NaCl window was preheated to 90°C and a thin film of resin was placed on the cell. Neat BF_3–MEA samples were first dissolved in methyl ethyl ketone (MEK), then cast onto NaCl plates.

The diglycidyl ether of bisphenol-A (DGEBA) was obtained from Shell Chemical Co. (Houston, TX). After purification by recrystallization from methyl isobutyl ketone, it had a melting point of about 45°C. Experiments were performed on samples containing 2–66.4 parts BF_3–MEA per 100 parts by weight DGEBA (phr). These BF_3–MEA levels are the equivalent of 5.7–67 mol %.

Cure Mechanism

The cure mechanism was studied using ^{19}F and ^{1}H NMR and isothermal infrared spectroscopy to monitor the thermal conversion of BF_3–MEA, which occurs before the cross-linking reaction. Infrared spectroscopy and DSC were used to monitor the subsequent cross-linking reaction. The experiments were conducted on samples containing from 2 to 25 phr BF_3–MEA in DGEBA. Table I shows the conversions between phr, weight percent, and mol percent values for the concentrations of BF_3–MEA used.

Table I Phr, Weight Percent, and Mol Percent Equivalents of BF_3–MEA Used in Experiments

phr	Wt %	Mol % DGEBA
2	1.96	5.68
3	2.91	8.29
4	3.84	10.75
5	4.76	13.09
10	9.09	23.15
25	20.00	42.95

BF_3–MEA alone was used in the NMR experiments, which were performed on a 300 MHz General Electric instrument. For the proton spectra, 1 part of BF_3–MEA was dissolved in roughly 10 parts by weight of d_6-DMSO. The sweep width was 2304 Hz; the pulse width, 3 μs; the pulse delay, 8 s; and the acquisition time for 16,384 points, 1.78 s. For fluorine, as concentrated a solution as possible of BF_3–MEA in d_6-DMSO was used. The sweep width was 23,809.5 Hz; the pulse width, 6 μs, the pulse delay, 10 s; and the acquisition time for 16,384 data points, 688.13 ms. The field lock was set at 2.49 ppm (DMSO) for the proton spectra, and an internal reference of −163 ppm (C_6F_6) was used for the fluorine spectra.

Cure Kinetics

Samples of BF_3–MEA and BF_3–MEA/DGEBA containing 4, 10, and 25 phr hardener were cured isothermally in an IBM Instruments IR30S FTIR that was equipped with a 32 mm heated cell from Spectra-Tech. To minimize the temperature equilibration time when a sample was placed in the spectrometer, only one window was used in the heating cell. All spectra were collected from 4000 to 500 cm^{-1} at a resolution of 2 cm^{-1}. Fifteen scans were taken for each data point and the resulting interferogram was apodized using triangular apodization during the Fourier transform.[17]

The maximum time for the initial temperature equilibration was 180 s at 150°C. Thereafter, spectra were taken approximately every 90 s for 1 h. The epoxide concentration was monitored as a function of time and temperature, and the data were normalized to an initial epoxy concentration of 1.0 using the skeletal aromatic Ar—C—Ar stretch at 1184 cm^{-1}.[18,19] The conversion (α) was defined as 1 − (normalized concentration); the conversion increased from 0 at the beginning of the reaction to 1 when the epoxy concentration decreased to 0:

$$\text{Normalized concentration} = \frac{[\text{Area}(916)/\text{Area}(1184)]_{t=\tau}}{[\text{Area}(916)/\text{Area}(1184)]_{t=0}} \quad (1)$$

and Area( ) is the area of the IR peak at that wavenumber. The concentration/time curves for DGEBA were generated by monitoring the area of the epoxy peak with time and temperature. The il-

lustration below indicates how base lines were determined for the peak integrations:

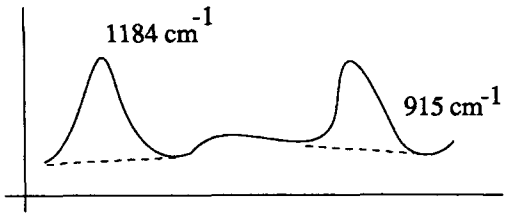

DSC kinetics experiments were carried out under nitrogen on epoxy samples containing 2, 3, 4, and 5 parts per 100 (phr) by weight of BF_3–MEA. The sample powders were ground then intimately mixed without heating. After the samples had been weighed out into DSC pans, the pans were kept in a freezer until needed. The heating rates were 2.5, 3.5, 5, 7, 8.5, 10, 13, and 15 K/min. over a temperature range from 25 to 250°C. Sample sizes were about 10 mg. The DSC conversion α_{DSC} is defined as

$$\alpha_{DSC} = 1 - \frac{\Delta H_{residual}}{\Delta H_{total}} \quad (2)$$

where $\Delta H_{residual}$ is the heat of reaction and ΔH_{total} is the total heat of reaction determined by a scan from room temperature to 250°C.

Cross-linking systems, in particular those that have high functionality reactants, usually do not react completely.[9] Hence, the classical Borchardt–Daniels kinetic analysis method[13] may yield values of the activation energy (E_a) and the preexponential factor (A) that are over 70% above their actual values.[9] To determine these parameters accurately, which is essential for any kinetic modeling, the exotherm peak shift method[11,14,15] was used.

RESULTS AND DISCUSSION

BF_3–MEA Thermal Breakdown

The thermal breakdown of BF_3–MEA was monitored with isothermal FTIR and NMR experiments. For FTIR experiments, a spectrum was taken at room temperature; then the cell was heated to 132°C and scans were made repeatedly for 1 h at 132°C. Finally, the cell was cooled to room temperature and a last scan was made. The FTIR spectra are shown in Figures 1–3.

Figure 1 shows the IR spectrum of BF_3–MEA at room temperature. The peaks at 3297 and 3268 cm^{-1} are due to asymmetric and symmetric NH stretching vibrations.[18] The bands around 3000 cm^{-1} are caused by CH stretching. CH symmetrical bending vibrations appear near 1375 cm^{-1}, whereas asymmetrical vibrations occur near 1475 cm^{-1}. The band at 1620 cm^{-1} is caused by NH bending. The peaks at 1145 and 945 cm^{-1} (Fig. 2) are caused by BF asymmetric and symmetric stretching in BF_3.[19] The peak at 1044 cm^{-1} is caused by BF_4^-.[20] The presence of this band indicates that, even after washing, a small amount

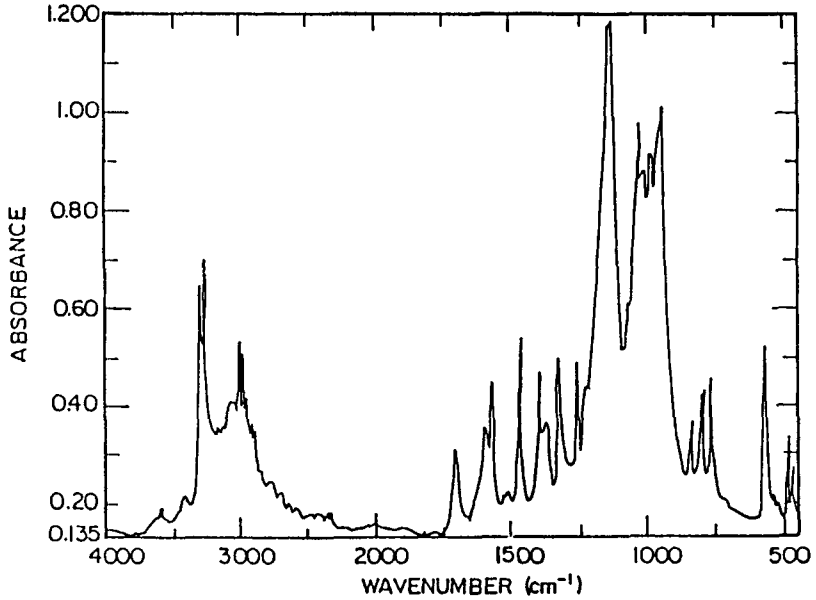

Figure 1 IR spectrum of BF_3–MEA at 25°C.

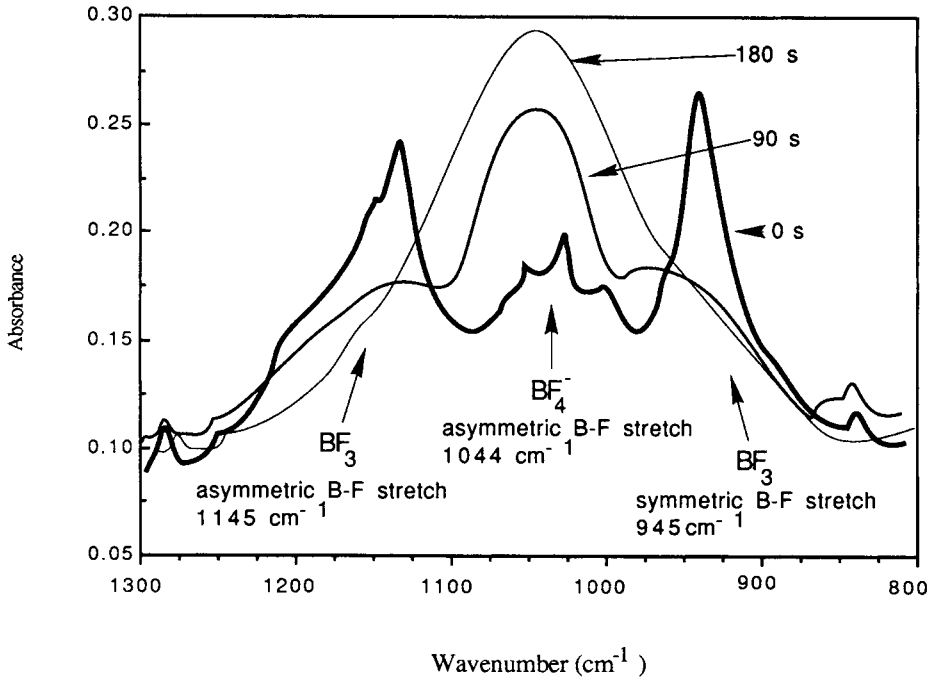

Figure 2 IR spectra at 132°C of BF_3–MEA showing changes in BF_3 and BF_4^- absorbances.

of fluoroboric acid remains in the specimen. The BF_4^- peak merges into a peak at 920 cm^{-1}, which is characteristic of aliphatic amines. The spectra in Figure 2 show the changes in the BF absorbances at 132°C. The BF_3 peaks broaden and decrease rapidly with heating, while the BF_4^- peak grows larger. This is consistent with the conversion of BF_3–MEA to HBF_4.

Figure 3 shows the IR spectrum of the sample after cooling to room temperature. The BF_4^- peak is still very strong, indicating that the reaction that produced it may be irreversible. The features at 3000 cm^{-1} are changed somewhat in that the CH stretch is clearly visible, whereas the NH absorbances are not. The peaks of the room temperature spectrum are quite sharp, showing the effects of thermal

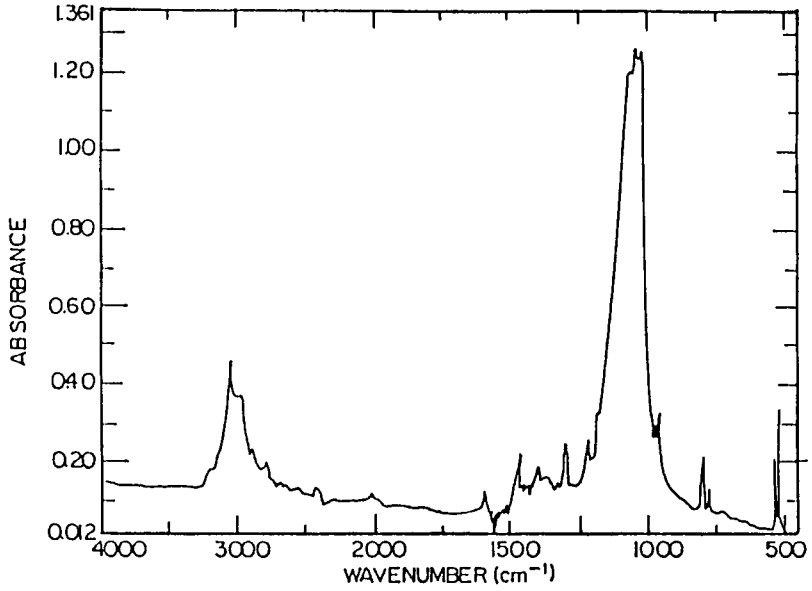

Figure 3 IR spectrum at 25°C of BF_3–MEA after 1 h at 132°C and cooling to 25°C.

broadening at elevated temperature. The peaks that were present between 1200 and 1750 cm^{-1} have either disappeared or are greatly diminished in size. This is unexpected and may be indicative of a low-boiling component, such as ethylamine, being vaporized from the open cell.

The change in the BF_4^- peak height with time is shown in Figure 4. The data are normalized to the highest absorbance of BF_4^- observed during the experiment. The data show that at 132°C there is a rapid increase in the BF_4^- anion concentration. In addition to the rapid thermal breakdown of BF_3–MEA, the infrared studies show the persistence of the fluoroborate anion. This observation is in agreement with the findings of Smith et al.[10,11] and Smith and Smith.[12]

For the NMR studies, the BF_3–MEA was dissolved in deuterated DMSO (d_6-DMSO) and a temperature ramp was applied. Starting from 25°C, the temperature was increased slowly to 80°C. The proton spectra used residual ^1H in the DMSO for the reference; an external reference of hexafluorobenzene (C_6F_6) was used for the fluorine runs.

The room temperature proton spectrum of BF_3–MEA dissolved in d_6-DMSO is shown in Figure 5. Given the chemical structure of BF_3–MEA, three peaks are expected, but six peaks are visible in the spectrum. The multiplet at 1.1 ppm is caused by CH_3. It is composed of two superimposed triplets and indicates the presence of two different alkyl species. The peak at 2.49 is due to DMSO. This was proved by changing the solution concentration and observing that this was the only peak whose relative size changed with respect to the others. There are two quartets at 2.8 and 2.6 ppm. These are caused by CH_2 and are due to the two different species mentioned in relation to the methyl peaks. There is a peak at 6.2 ppm that is caused by a proton attached to a nitrogen and another broad peak at about 7.3 ppm. Happe et al.[13] observed these two families of peaks and attributed them to $BF_3—NH_2C_2H_5$ and $BF_4^-—NH_3^+C_2H_5$.

The $BF_4^-—NH_3^+C_2H_5$ is the minor component in fresh BF_3–MEA. These peaks have the expected 3 : 2 : 2 CH_3 : CH_2 : NH_2 relationship to each other. The presence of a BF_4 species is consistent with the IR observations that BF_4^- was present before heat treatment. The NMR data show that the BF_4 is present most probably as an amine salt, $BF_4^-—NH_3^+C_2H_5$. There is another peak whose origin is not clear. The peak at 3.4 ppm broadens and disappears rapidly upon heating. It does not reappear when the sample is cooled; this peak may be caused by water. Figure 6 shows the proton spectrum at 80°C. Although the CH_3 multiplet looks the same as before, the CH_2 peaks have changed significantly. The CH_2 : CH_3 ratio changes from 1 : 13 at room temperature to 1 : 3 at 80°C, indicating conversion to $BF_4^-—NH_3^+C_2H_5$, even at 80°C. The peak at 3.4 ppm has almost disappeared and is shifted upfield slightly. The peak caused by the nitrogen protons has also shifted upfield and is now a little broader.

After cooling to room temperature, the spectrum remained unchanged, indicative of an irre-

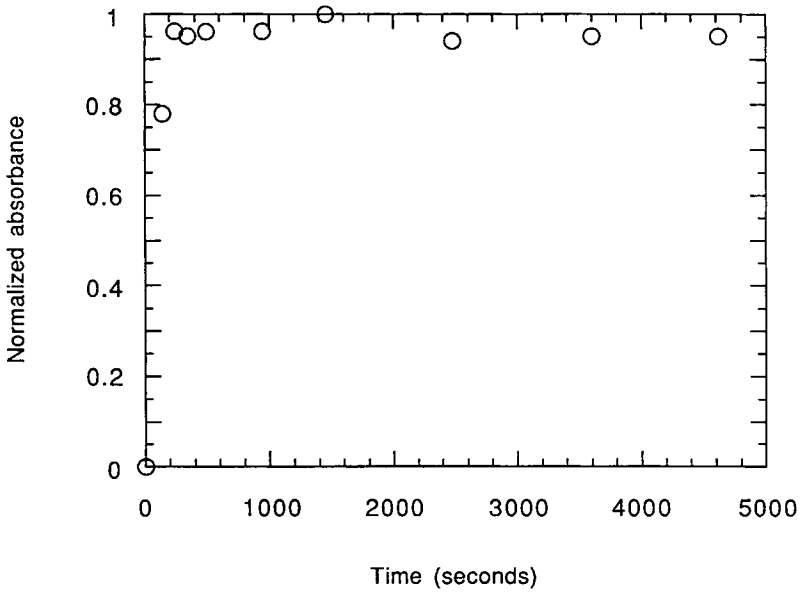

Figure 4 Normalized 1044 cm^{-1} BF_4^- absorbance as a function of time at 132°C.

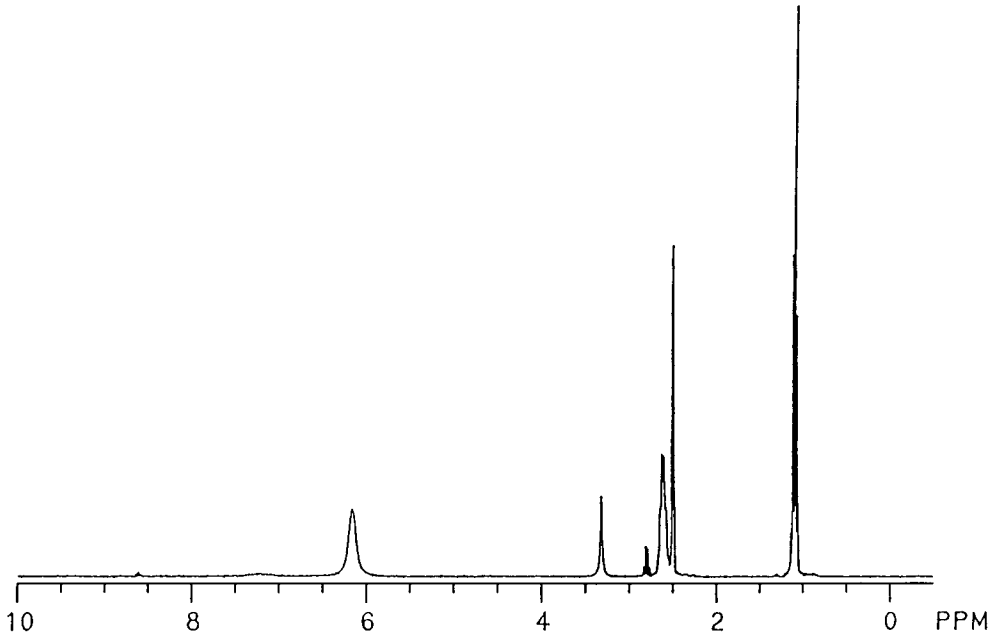

Figure 5 Proton NMR spectrum of BF_3–MEA at 25°C.

versible reaction that converted BF_3–MEA to $BF_4{-}NH_3C_2H_5$. The proton NMR data do not agree with the conclusions of Happe et al.,[13] who observed no change in their BF_3–MEA samples even after annealing at 139°C for 1 h. Here, changes were observed at 80°C.

Figures 7 and 8 show two ^{19}F spectra taken at room temperature and at 80°C. There are four peaks visible in both spectra: The quartet centered about −149 ppm caused by BF_3; the quartet caused by BF_4^- at −148.5 ppm; a singlet at −148.4 ppm; and a quartet at −140.1 ppm. The difference between the two spectra again is the increase in the BF_4^- peak with temperature. All three quartets were observed by Happe et al.[13] and Smith et al.[10] There is no question about the source of the quartets at −149 and

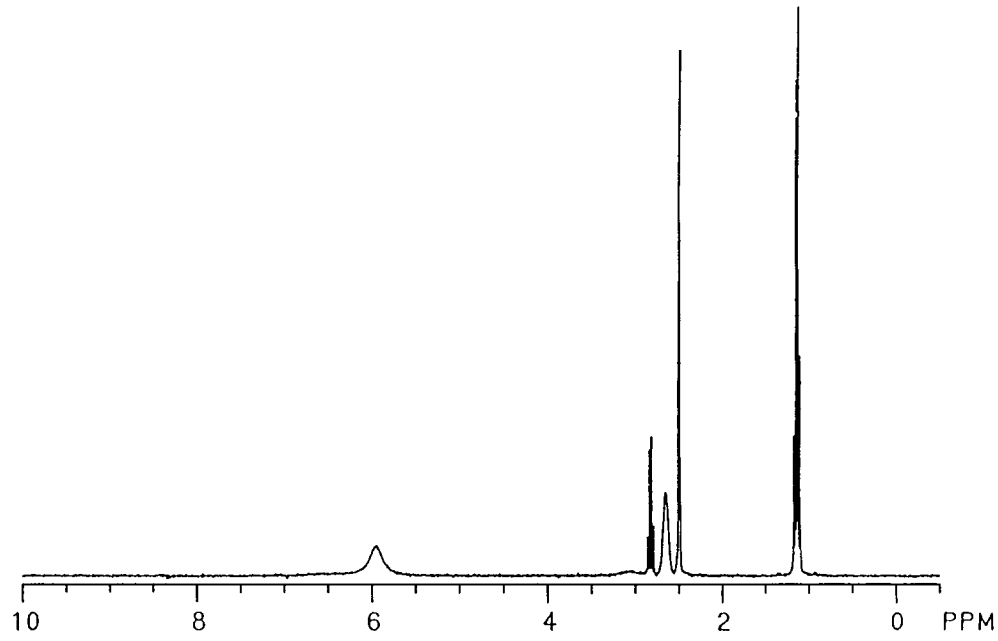

Figure 6 Proton NMR spectrum of BF_3–MEA at 80°C.

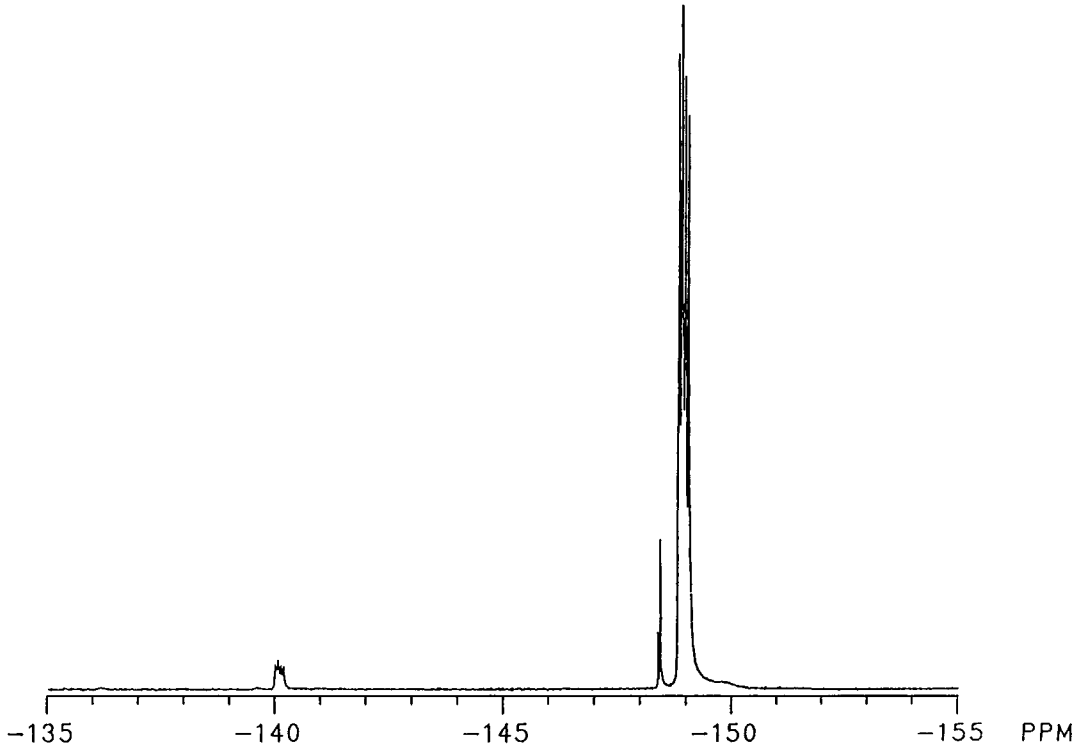

Figure 7 ^{19}F-NMR spectrum of BF_3–MEA at 25°C.

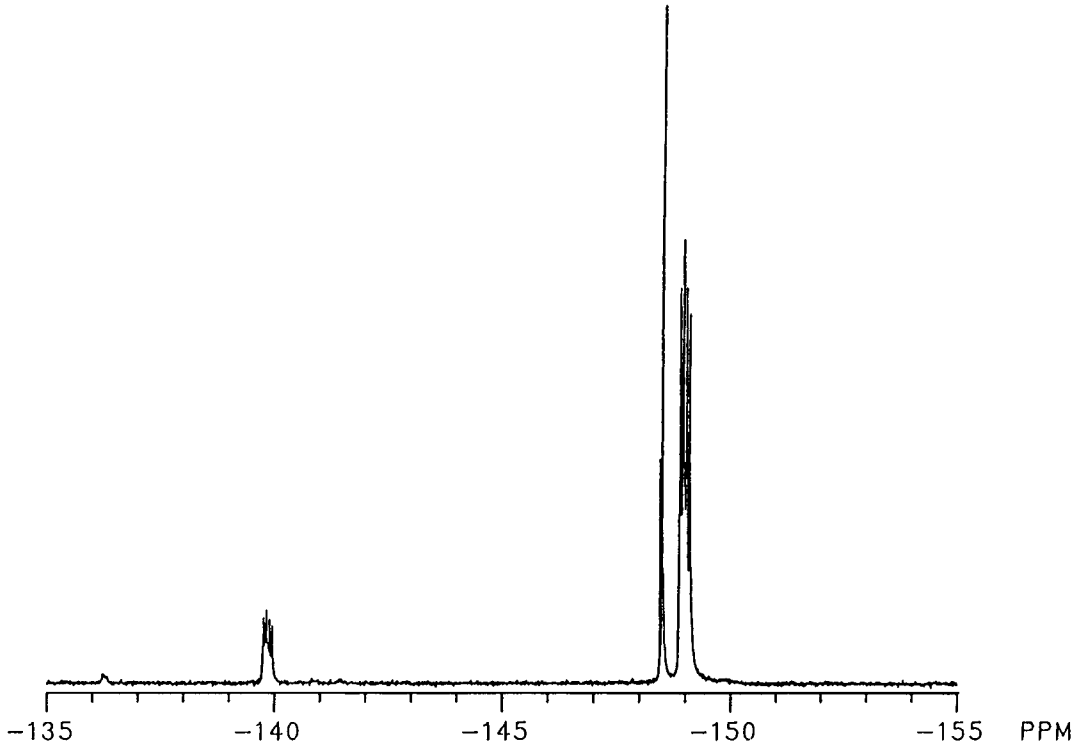

Figure 8 ^{19}F-NMR spectrum of BF_3–MEA at 80°C.

−148.5 ppm, but Smith et al. attribute the peak at −140.1 ppm to a complex of BF_3 and DMSO, whereas Happe et al. suggest that it is caused by $HBF_3(OH)$.

Smith et al.[11] and Smith and Smith[12] found that, above 80°C, BF_3–MEA was converted into HBF_4 in less than 5 min. They concluded that given the typical cure conditions for an epoxy (temperatures of 120–180°C), the BF_3–MEA would be completely converted to HBF_4 before the cross-linking reaction began in BF_3–MEA/epoxy systems. In contrast to Smith et al., Happe et al.[13] observed a slow conversion of BF_3–MEA into a mobile salt that was the catalytic agent for the epoxy; they state that BF_3–MEA is converted to a monoboroester as proposed by Landau.[1] During this reaction, HF is released, and the HF combines with another molecule of BF_3–MEA to form $BF_4^- — NH_3^+C_2H_5$.

The results presented here are in agreement with the findings of Smith et al.[10] and Smith and Smith.[12] The rapid thermal breakdown of BF_3–MEA into a BF_4^- containing species was observed. The data support the mechanism whereby 2 mol of BF_3–MEA react to form 1 mol of the catalytically active species in a rapid, thermally activated reaction.

Complex Formation and Epoxy Etherification

Samples of BF_3–MEA/DGEBA containing 4, 10, and 25 phr BF_3–MEA were tested isothermally in the FTIR. The concentration/time curves for DGEBA were generated by monitoring the area of the epoxy peak with time and temperature.

There is a rapid formation of OH groups during the initial heat-up period. An expanded spectral region from 3100 to 3700 cm^{-1} representing the OH and NH absorbances is shown in Figure 9. The data are from a sample containing 10 phr BF_3–MEA heated at 120°C. The OH absorbance at 3550 cm^{-1} increases so rapidly from zero at the beginning of the cure that hydroxyl formation takes place while the FTIR heated cell temperature is coming to equilibrium. The NH absorbances at 3160 and 3260 cm^{-1} decrease rapidly initially, but thereafter decrease very slowly. Surprisingly, these peaks persist even after 32 min of reaction. The two peaks represent the antisymmetric and symmetric stretching modes of the NH vibrations. During the OH-formation period, the peak corresponding to the aliphatic ether was not observed (Fig. 10), indicating that although the thermal breakdown and complex formation reactions were occurring no etherification was taking place. After the complex forms, there is a much longer period during which the epoxy homopolymerizes. During this period, the 1140 cm^{-1} absorbance of the aliphatic ether was observed. Because this peak occurs in the "signature" region of the spectrum, along with a number of other overlapping peaks, it was not possible to perform a quantitative analysis on it.

It is believed that cross-linking through the secondary —OH groups is not taking place to a significant degree. In studies of similar systems, Kakurai and Noguchi[21] found that the OH/epoxy reaction occurred only at high temperatures. Schechter et al.[22,23] found that temperatures of 200–250°C were

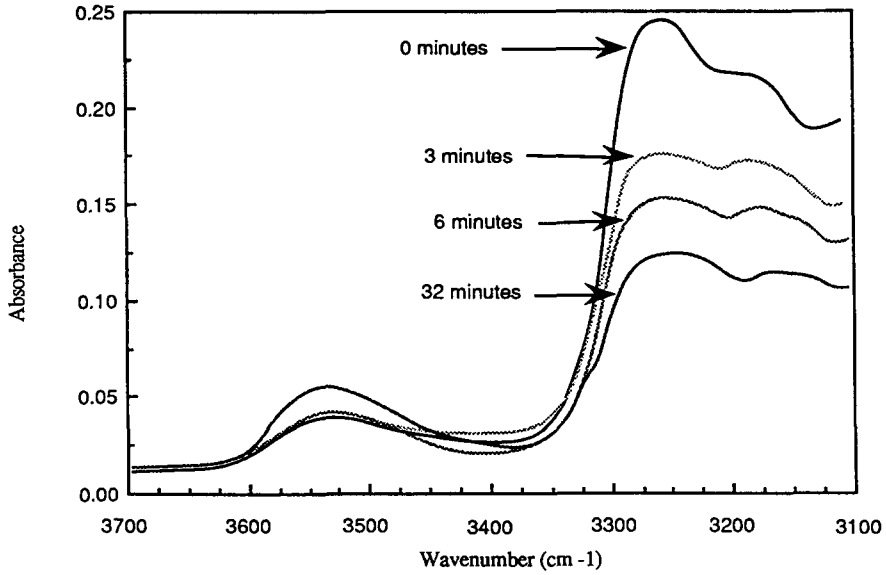

Figure 9 Changes in OH and NH absorbances with time for a 10 phr sample at 120°C.

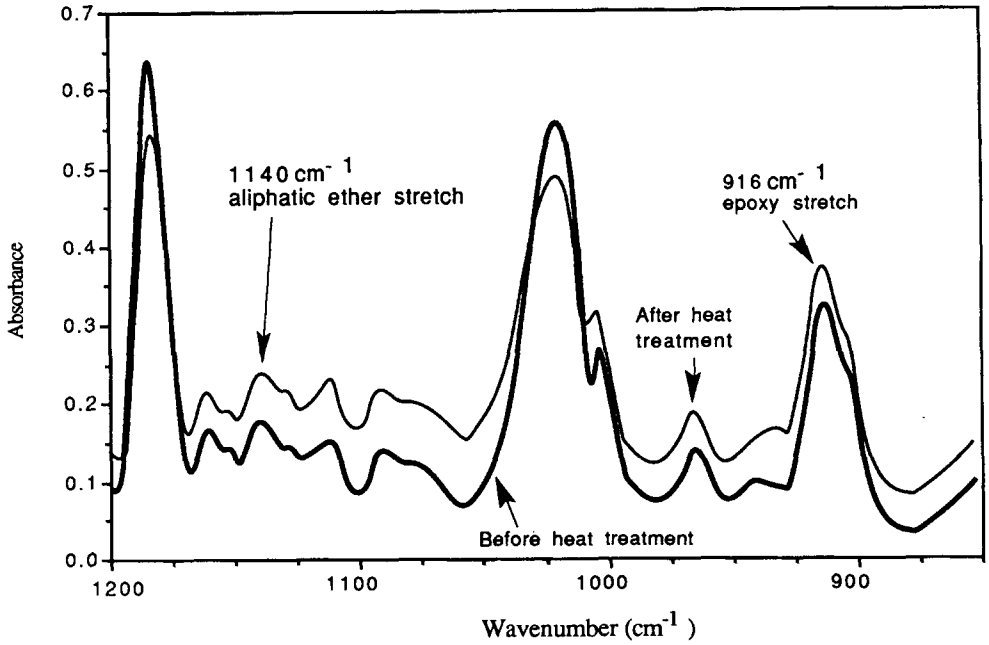

Figure 10 FTIR spectra of a 4 phr BF_3–MEA/DGEBA sample before and after the complex formation reaction.

required for this reaction and that the reactivity of the OH decreased with substitution of the alcohol.

The cationic polymerization of epoxy molecules occurs through the terminal carbon atom.[24] In this case, HBF_4 opens an epoxide ring to form a protonated oxonium ion, which yields an activated monomer. The initial OH absorbance observed in the FTIR spectra is due to this reaction. The activated monomer polymerizes other epoxy groups, with the BF_4^-, a nonnucleophilic anion, associated with the oxygen. Because the BF_3–MEA is converted to HBF_4, the reaction is not initiated by a boroester. Furthermore, carbon–fluorine absorbances (at 1100–1000 cm^{-1}) were not observed in the FTIR spectra. The thermal breakdown of BF_3–MEA has been shown to be rapid and irreversible with temperature, yielding a stable product.

After the complex formation, the etherification reaction proceeds. Figure 11 shows the normalized concentration data for a 4 phr BF_3–MEA/DGEBA

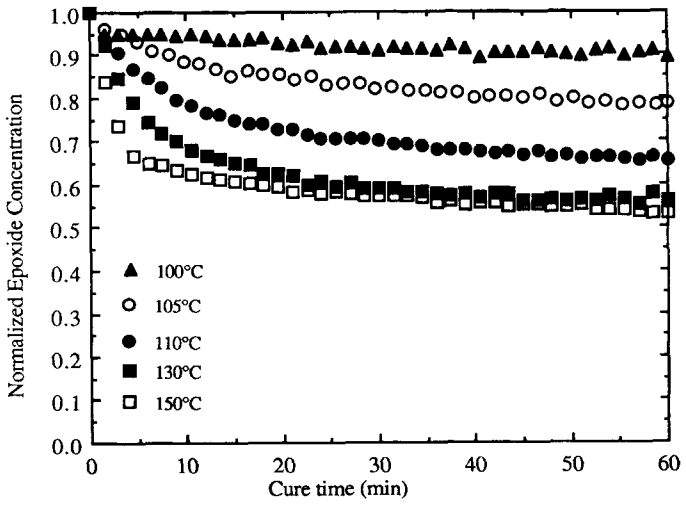

Figure 11 Normalized concentration profiles for a 4 phr BF_3–MEA/DGEBA mixture.

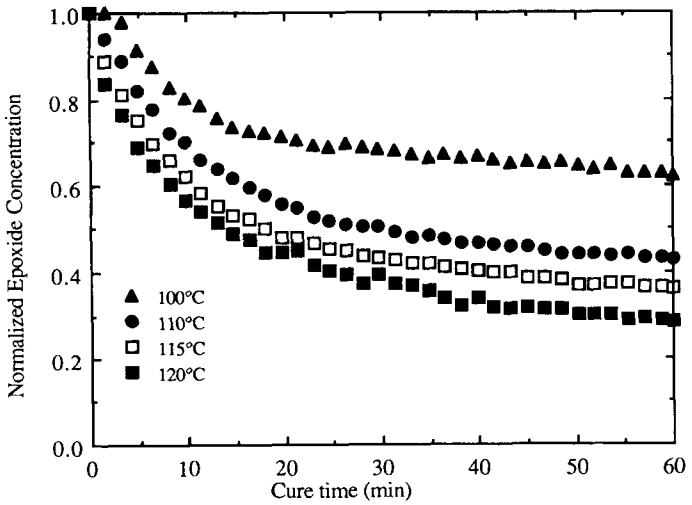

Figure 12 Normalized epoxy concentration profiles for a 10 phr BF_3–MEA/DGEBA mixture.

mixture, and Figure 12 shows the results for a mixture containing 10 phr BF_3–MEA. In both instances, the concentrations decrease steadily over the course of the reaction, although the reaction rates decrease noticeably as the reaction progresses. The plots of normalized epoxy concentration vs. time therefore exhibit two regions, the positions of which depend on the reaction temperature and the accelerator concentration. In the first region, which occurs at the beginning of the reaction, the epoxy concentration decreases quite rapidly. In the second region, the reaction rate is considerably slower. At 4 phr, the reaction rate decreases after 25 min at 130°C, whereas with 25 phr BF_3–MEA, the second region was not entered until after 50 min, even at 110°C.

Isothermal DSC experiments were performed at 110°C on 4 and 25 phr BF_3–MEA mixtures to establish whether or not vitrification caused the reduction in the reaction rate. After completion of the isothermal cure, the samples were rescanned from −50 to 250°C at 10 K/min. The results are plotted in Figure 13. They show that, for both concentra-

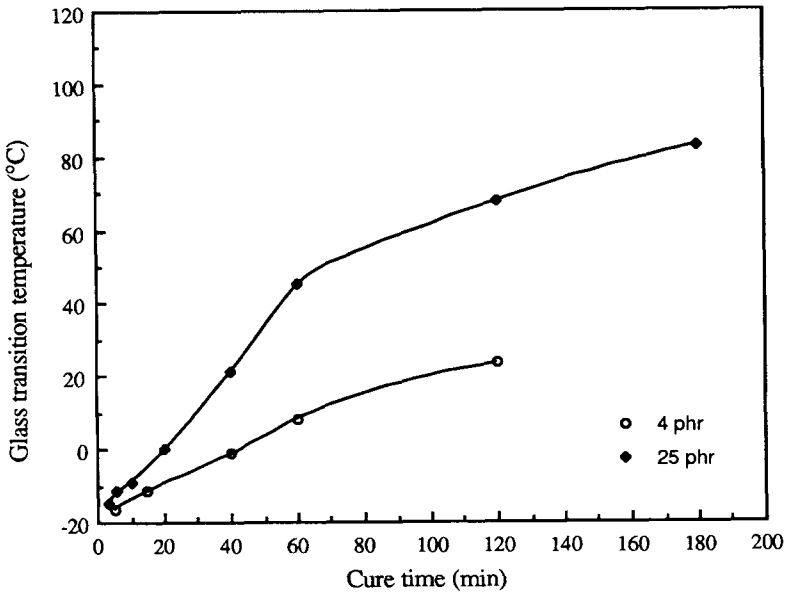

Figure 13 Glass transition temperature vs. cure time at 110°C for 4 and 25 phr BF_3–MEA/DGEBA mixtures.

tions, the T_g is lower than the cure temperature of 110°C, even after 180 min. In the case of the 4 phr samples, the T_g after 60 min is 8.3°C. Since the 4 phr FTIR experiment showed a significant reduction in reaction rate after only 20 min at 110°C, clearly, vitrification is not the cause for the observed rate decreases.

The marked decrease in reaction rate even at low epoxy concentrations can be explained by steric inhibition of the reactants; as the network gets tighter, the reacting molecules are unable to approach each other closely enough to react. The final extent of reaction is therefore determined by how many chains are reacting and by the reaction temperature.

As shown in Figure 14, three features were common to all the DSC traces. First, there is an endothermic peak at 45°C that is caused by the melting of the DGEBA. At 110–120°C, there is a small exotherm, followed by a much larger exotherm with a peak between 150 and 175°C.

To determine whether the small exotherm was caused by the thermal breakdown of BF_3–MEA, a sample of BF_3–MEA was scanned in the DSC over a temperature range of 45–150°C at 10 K/min. A melting peak was observed at 85°C, and a small exotherm of 35 J/g followed the melting peak very closely. This exotherm may be due to the thermal conversion of BF_3–MEA to HBF_4, a reaction that was observed in both the FTIR and NMR experiments.

The heat-treated BF_3–MEA from the dynamic DSC experiment was used to prepare a 25 phr mixture with DGEBA. Since the BF_3–MEA had already undergone thermal conversion to HBF_4, both the melting and HBF_4 formation peaks would be absent from the DSC traces. The experimental conditions were 45–250°C at 10 K/min. Two exotherm peaks were observed: The first peak is assigned to the formation of the complex of HBF_4 and DGEBA, and the second, larger peak is caused by etherification. These assignments are consistent with the mechanism of complex formation and epoxy curing. As expected, there is no endotherm peak, signifying a complete conversion of BF_3–MEA in the prior heat treatment.

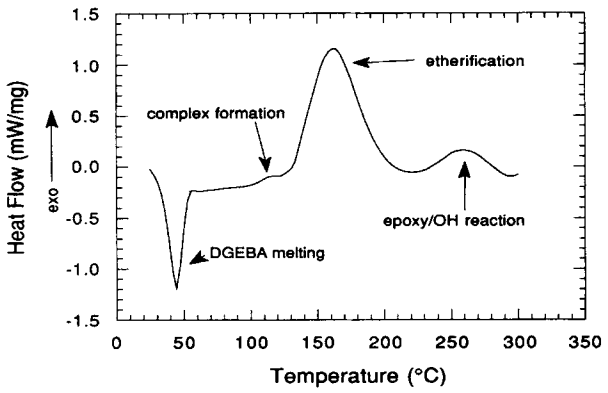

Figure 14 DSC thermogram of a 4 phr BF_3–MEA/DGEBA sample that was cured at 10 K/min to 325°C.

A 4 phr BF_3–MEA sample was heated in the DSC at 10 K/min to 325°C. The purpose in performing the dynamic scan was to determine if the OH/epoxy reaction could be resolved from the epoxy/epoxy etherification. The data are plotted in Figure 14 with the important features marked with arrows. There are four items of note in the DSC scan: At 45°C, there is the expected melting of DGEBA. At 120°C, there is a small peak caused by the formation of the HBF_4/epoxy complex. The epoxy/epoxy etherification peak occurs at 165°C, and, finally, there is a broad flat peak at 258°C, caused by the OH/epoxy reaction. The heat evolved in the etherification was 304.4 J/gm, whereas the heat evolved in the OH/epoxy reaction is 51.4 J/gm. The data support the conclusions of Kakurai and Noguchi[21] and Schechter et al.[22,23] that the OH/epoxy reaction occurs above 200°C.

The assignment of the peak in Figure 14 labeled "complex formation" was verified in the following manner: A DGEBA sample containing 4 phr BF_3–MEA was conditioned in the DSC by heating at 5 K/min to 125°C, the temperature just below that at which the epoxy etherification starts but above the temperature for the thermal conversion of BF_3–MEA to HBF_4. The sample was analyzed in the FTIR both before and after heat treatment to determine if the epoxy etherification reaction had initiated. No change in the 1140 cm^{-1} aliphatic ether stretch was found. The 1140 cm^{-1} peak increases during the curing of the resin, and, therefore, is a good indicator of etherification. The reaction mechanism upon which the subsequent kinetics experiments were predicated is shown in Figure 15.

Etherification Kinetics

Dynamic DSC indicated that there were two exotherms present: The first exotherm is caused by the complex of HBF_4 and DGEBA, and the second is caused by etherification.[1] The complex formation peak is very small, while the etherification peak is quite large. The size of the peak increased over the 2–5 phr BF_3–MEA concentration range used in the experiments.

The results of the DSC peak-shift calculations are given in Tables II and III. Both tables show the

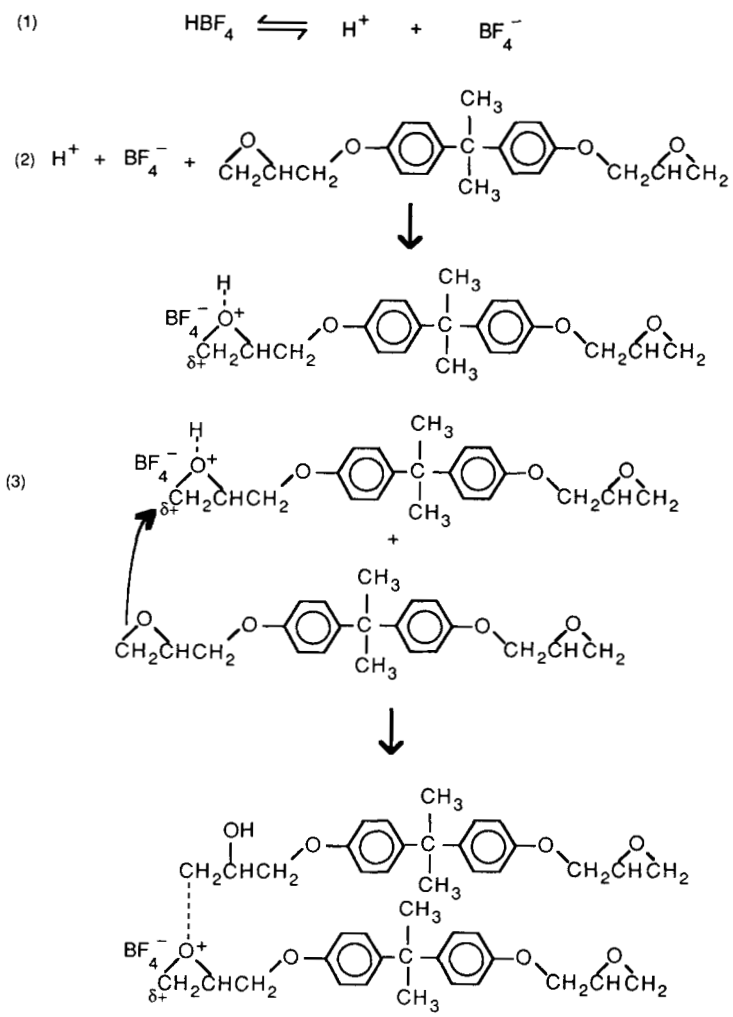

Figure 15 Complex formation and etherification mechanisms.

preexponential factors and the activation energies as functions of the BF_3–MEA concentration in phr. Table II shows the results for the etherification reaction, and Table III shows the corresponding results for the complex formation reaction.

The average value of the activation energy for the etherification reaction was determined to be 87.9 kJ/mol. As expected, the activation energy does not change with accelerator concentration. In contrast to the activation energy, the preexponential factor increases as the initial BF_3–MEA concentration increases. The increase in the preexponential factor is indicative of the greater number of active sites for reaction caused by the increasing concentrations of BF_3–MEA.

Table II Summary of DSC Kinetic Parameters for Etherification Reaction

BF_3–MEA (phr)	A (s^{-1})	E_a (kJ/mol)
2	1.40E8	85.5
3	2.30E8	87.0
4	3.08E8	89.6
5	3.10E8	89.8

Table III Summary of DSC Kinetic Parameters for BF_3–MEA/DGEBA Complex Formation Reaction

BF_3–MEA (phr)	A (s^{-1})	E_a (kJ/mol)
4	1.25E9	80.4
5	1.20E9	81.6

The kinetic parameters for the complex formation (BF_3–MEA/epoxy) were calculated in a similar manner. The activation energy for the complex formation reaction was 81 kJ/mol, and the preexponential factor was 1.23×10^9 s^{-1}, as indicated in Table II.

The kinetic parameters for the BF_3–MEA/epoxy complex reaction were only determined for the 4 and the 5 phr BF_3–MEA samples because the exotherm peaks with 2 and 3 phr BF_3–MEA were too small to be distinguishable from the etherification peak.

An analysis of the heat-flow equation for the DSC showed that the thermal lag between the sample and reference pans had a very small effect on the peak exotherm positions.[25] The analysis showed that the Kissinger and Ozawa method could be applied to obtain the kinetic parameters from the DSC data generated here.

In addition to the dynamic DSC experiments, isothermal IR experiments were run on the 4, 10, and 25 phr BF_3–MEA/DGEBA mixtures at temperatures ranging from 100 to 150°C. The wide range of experimental conditions and reactant concentrations provided information about the activation energy, the preexponential factor, and the reaction order of the etherification reaction.

Kinetic expressions for an n-th order irreversible reaction of the form

$$\frac{dC}{dt} = -KC^n \qquad (3)$$

were used to analyze the experimental data. In eq. (3), C is the reactant concentration; t, the time; K, the rate constant; and n, the reaction order. For a first-order reaction, rewriting the rate constant and integrating this expression from time t_0 to time t and from concentration C_0 to C gives

$$\ln\left(\frac{C}{C_0}\right) = A \exp\{E_a/RT\}(t_0 - t) \qquad (4)$$

where C_0 is the reactant concentration at time t_0. C_0 was taken as the normalized epoxy absorbance at 915 cm^{-1} after the temperature had stabilized in the IR heated cell upon heating from 90°C. The time varied from 2 s at 100°C to 160 s at 150°C. The result of this time delay is the inability to detect all of the initial epoxy decrease caused by the formation of the complex. The effect is minimal; however, at 4 phr BF_3–MEA, where the highest temperatures were used, a theoretical maximum of 2.9% of the epoxy is consumed in the complex formation reaction. At 25 phr BF_3–MEA, the highest temperature used was 110°C. Changing the BF_3–MEA concentrations and reaction temperatures in this manner resulted in very consistent data over the experimental conditions studied.

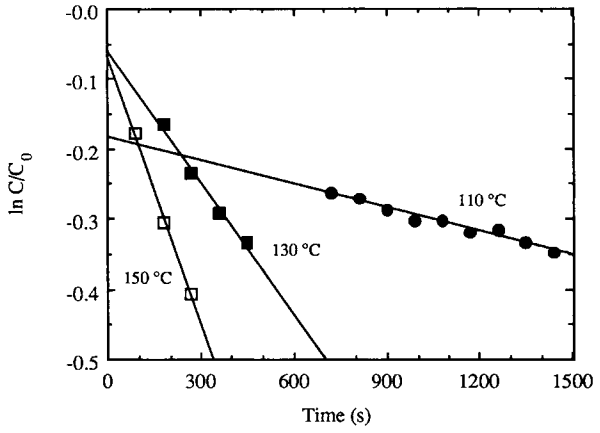

Figure 16 ln (C/C_0) vs. time for 4 phr BF_3–MEA/DGEBA.

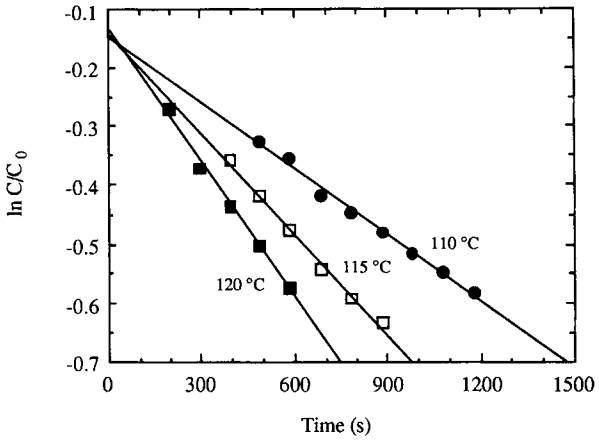

Figure 17 ln (C/C_0) vs. time for 10 phr BF_3–MEA/DGEBA.

Figures 16 and 17 show the first-order kinetic analysis plots for 4 and 10 phr BF_3–MEA concentrations. Both figures show $\ln(C/C_0)$ plotted against time. Straight lines with correlation coefficients of .97–.99 were obtained, signifying that the etherification reaction is pseudo-first order with respect to epoxy. Since there are a fixed number of BF_3–MEA molecules, the number of complexes formed will be constant throughout the polymerization and, therefore, the reaction should be pseudo-first order with respect to the epoxy.

The pseudo-first-order curing kinetics occurs because the etherification reaction is preceded by the

rapid complex formation reaction. The complex sites are regenerated whenever they react with an epoxy group; therefore, the result of the regeneration is a constant number of complex sites. This reaction scheme is illustrated below:

$$HBF_4 + E \xrightarrow{k_d} E^* \text{ fast} \quad (5)$$

where E represents an epoxy group, E^* represents an activated (complexed) epoxy group, and k_d is the rate constant for the complex formation. The polymerization step is shown in eq. (6). Here, k_p is the rate constant for the polymerization reaction:

$$E^* + E \xrightarrow{k_p} E^* \quad (6)$$

The kinetic equation for the etherification reaction can then be written as in eq. (7):

$$\frac{d[E]}{dt} = -k_p[E][E^*] = -k_p[E]\frac{[BF_3\text{–MEA}]}{2} \quad (7)$$

The slopes of the lines in Figures 16 and 17 were used to calculate preexponential factors. An activation energy of 82.5 kJ/mol was obtained for the etherification reaction for 4 phr BF_3–MEA, and a value of 89.4 kJ/mol was obtained for the 10 phr samples. These values agree with the value of 87.9 kJ/mol that was obtained from the dynamic DSC experiments. Preexponential factors calculated for the 4 and 10 phr data along with the DSC results are plotted with respect to BF_3–MEA concentration in Figure 18. Again, there is good agreement between the DSC and IR results.

The BF_3–MEA/DGEBA system exhibits a window where the etherification reaction is pseudo-first order. The position of this window in time–temperature space depends on the BF_3–MEA concentration. The kinetic equation,

$$\frac{d\alpha}{dt} = 1.2 \times 10^8 \frac{[BF_3\text{–MEA}]_0}{2} \times \exp\{-87.9/RT\}(1-\alpha)\ s^{-1} \quad (8)$$

where α is the conversion of epoxy groups and $[BF_3$–$MEA]_0$ is the initial concentration of accelerator in parts per 100 of epoxy, was derived from these experiments. Note that the activation energy is in kJ/mol.

CONCLUSIONS

NMR, FTIR, and DSC experiments were used to delineate the mechanisms for the BF_3–MEA/DGEBA homopolymerization reaction. BF_3–MEA undergoes a rapid thermal conversion to HBF_4, which is the catalytic species. This finding agrees with the conclusions of Smith and Smith.[12]

After the thermal conversion, there is a fast complex formation reaction between HBF_4 and the

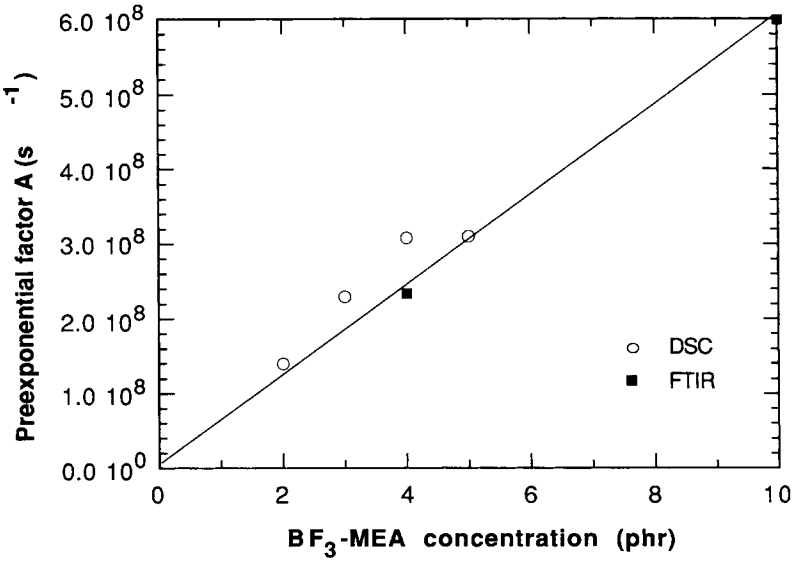

Figure 18 Dependence of preexponential factor A on BF_3–MEA concentration.

epoxy, which produces OH absorbances in the FTIR spectrum, and a carbocation from which the epoxy homopolymerization proceeds. An interesting and unanticipated effect of this curing mechanism is that the reaction rate is very sensitive to the accelerator concentration and the reaction temperature. At 4 phr BF_3–MEA, the reaction slowed noticeably after 45% of the epoxy had been converted, even though the reaction temperature was about 90°C above the T_g of the formed polymer. These observations indicate a system where polymerization proceeds from comparatively few "activated" chain ends, with the unactivated epoxy monomer continuously adding to the chains throughout the reaction.

REFERENCES

1. A. J. Landau, *Org. Coatings Appl. Polym. Sci. Proc.*, **42,** 299 (1964).
2. J. J. Harris and S. C. Temin, *J. Appl. Polym. Sci.*, **10,** 523 (1966).
3. J. D. Edwards, W. Gerrard, and M. F. Lappert, *J. Chem. Soc.*, 348 (1957).
4. R. Robinson, *TETRA*, **5,** 96 (1959).
5. R. J. Arnold, *Mod. Plast.*, **41,** 149 (1964).
6. Shell Chemical Co., *EPON Resin Structural Reference Handbook*, Shell Chemical Co., Houston, TX, 1983.
7. C. A. Kraus and E. H. Brown, *J. Am. Chem. Soc.*, **51,** 2690 (1929).
8. J. F. Brown, Jr., *J. Am. Chem. Soc.*, **74,** 1219 (1952).
9. C. A. Brown, E. L. Muetterties, and E. C. Rochow, *J. Am. Chem. Soc.*, **76,** 2537 (1954).
10. R. E. Smith, F. N. Larsen, and C. L. Long, *J. Appl. Polym. Sci.*, **29,** 3698 (1984).
11. R. E. Smith, F. N. Larsen, and C. L. Long, *J. Appl. Polym. Sci.*, **29,** 3713 (1984).
12. R. E. Smith and C. H. Smith, *J. Appl. Polym. Sci.*, **31,** 929 (1986).
13. J. A. Happe, R. J. Morgan, and C. M. Walkup, *Compos. Technol. Rev.*, **8,** 77 (1986).
14. C. S. Chen and E. M. Pearce, *J. Appl. Polym. Sci.*, **37,** 1105 (1989).
15. P. Kubisa, *Makromol. Chem. Macromol. Symp.*, **13/14,** 203–210 (1988).
16. P. Kubisa and R. Szymanski, *Makromol. Chem. Macromol. Symp.*, **3,** 203–222 (1986).
17. C. T. Foskett, in *Transform Techniques in Chemistry*, P. R. Griffiths, Ed., Plenum Press, New York, 1983, p. 11.
18. R. B. Silverstein, G. C. Bassler, and T. C. Morrill, *Spectrometric Identification of Organic Compounds*, Wiley, New York, 1981, p. 73.
19. G. Socrates, *Infrared Characteristic Group Frequencies*, Wiley, New York, 1980, p. 132.
20. C. J. Pouchert, Ed., *The Aldrich Library of Infrared Spectra*, 2nd ed., The Aldrich Chemical Co., Milwaukee, WI, 1975, p. 204.
21. T. Kakurai and T. Noguchi, *J. Soc. Org. Synth. Chem. (Jpn.)*, **18,** 485 (1960).
22. L. Schechter, J. Wynstra, and R. E. Kurkjy, *I & EC*, **48,** 94 (1956).
23. L. Schechter, J. Wynstra, and R. E. Kurkjy, *I & EC*, **49,** 1107 (1957).
24. C. A. May, *Epoxy Resins: Chemistry and Technology*, 2nd ed., Marcel Dekker, New York, 1988, p. 339.
25. M. N. Tackie, PhD Thesis, Syracuse University, Syracuse, NY, 1989.

Received February 12, 1992
Accepted May 12, 1992